Identification of the operating parameters of the friction drum drive in industrial conditions

Indexed by:
Web of Science Group

Piotr Kulinowski [a], Piotr Kasza [a], Jacek Zarzycki [a]

[a] AGH University of Science and Technology, Al. Mickiewicza 30, 30-059 Krakow, Poland

Highlights

- Measurement of the friction coefficient in the laboratory cannot fully reflect the actual conditions.
- Characteristics of the operation of the drive-tensioning system allows for determining the slip limit.
- The mobile measuring system enables determining the conveyor's characteristics.
- A technique for measuring the operational friction coefficient of a drum drive has been developed.

Abstract

The publication presents the results of measurements of the operating parameters of the drum drive of a belt conveyor operating in a copper ore mine. The laboratory and industrial tests of belt conveyor components so far have largely focused on idler sets, the belt and the conveyor route. The authors of the publication notice that the subject literature lacks information on research into the coefficient of friction between the belt and the drum in an industrial facility under real conditions, which may imply that the phenomenon of driving force transmission from the drum surface to the belt has not been thoroughly explored. The investigations described in the publication were aimed at determining the kinetic coefficient of friction between the conveyor belt and the lining of the drive drum under operating conditions. In the first part of the study, preliminary laboratory tests were carried out, whereas in the second part of the study, a mobile, non-invasive measurement system was applied, which allowed for recording the kinematic and dynamic parameters of the conveyor's operation. During the several dozen minutes of the conveyor's operation, there were several start-ups and brakings as well as periods of steady operation under variable load on the material handled. The non-typical planned sequence of switching on the drive motors caused a temporary slip of the belt on the drive drum surface during one of the start-ups. The recorded parameters of the conveyor operation enabled determining the operational limit value of the friction coefficient between the belt and the lining of the drive drum.

Keywords

belt conveyor, friction coefficient, frictional contact, exploitation characteristics.

1. Introduction

Belt conveyors belong to the most effective means of transporting loose materials. Global trends in the development of the raw materials industry, in which conveyor transport systems are of crucial importance, force the design of ever longer and effective haulage routes. Modern belt conveyors should be characterized by high reliability and durability as well as low investment and operating costs.

Currently conducted research and development works in the field of conveyor belt transport include diagnostics and monitoring as well as laboratory and industrial tests. The knowledge and experience gathered during these investigations help to improve the calculation methods and optimize the conveyor design.

The use of advanced diagnostic and monitoring methods significantly contributes to the improvement of the reliability and safety of belt transport systems operation [17, 18, 26]. In [9], the authors indicate that the development of conveyor transport systems requires modern systems for monitoring the condition of components and effective diagnostic systems that implement the assumptions of Industry 4.0. One of the current trends in the development of conveyor transport is also the reduction of energy consumption through the use of speed control systems as a function of the degree of the conveyor's loading [6].

In the field of laboratory tests, particular attention is paid to the testing of conveyor components, such as idlers and belts [1]. The works carried out in this area confirm that the operational features of the conveyor's subassemblies may be determined in laboratory tests, provided that the actual operating conditions have been reproduced, for example the condition of the idler load with radial and axial forces when measuring the rotational resistance [11, 16].

Industrial testing of belt conveyors is a necessary element in the process of calculation methods verification. The publication [2] emphasizes the need to identify the load of the conveyor with material transported in real conditions, using dedicated specialized equipment. Measurements of conveyor operation parameters in industrial conditions are necessary to verify some calculation factors, such as the main resistance coefficient, which is discussed in the paper [4]. The results of properly planned and systematically conducted industrial tests provide a basis for introducing advanced, nonlinear computa-

tional models into design practice [7]. Tests conducted on real objects are used to optimize the key components of the conveyor, for example, the publication [12] presents the measurement of the condition of idler sets load, which was used to determine the optimal geometric parameters of the conveyor's route.

Currently, there are many IT tools available to support the process of designing belt conveyors. They use various calculation models, such as those specified in the CEMA and DIN 22101 standards, as well as proprietary methods developed in research centres, e.g. at the University of Hannover, Wrocław University of Technology or the AGH University of Science and Technology. All these methods require defining unambiguous input parameters, the values of which should be verified in laboratory and industrial tests on real objects. It is necessary as the comparison of the standard calculation methods used in the publication [20] shows significant discrepancies in the results.

Useful information on the functioning of belt conveyor transfer points is provided by the results of simulation tests employing the discrete element method [21]. The authors use the DEM environment to define guidelines for designing reliable chutes which ensure reduction of belt motion resistance, central feeding of mined rock and limitation of the process of mined rock defragmentation. Verified computational procedures and simulation models are applied to improve the efficiency of the conveyor's work by determining the most advantageous construction parameters of the belt [23, 24], correcting the spacing of idler supports [3] or through a proper selection of belt tensioning systems [5, 22].

In the world literature, there are no mentions of the results of research into the coefficient of friction between the belt and the drum carried out in an industrial facility, which may indicate that the phenomenon of the driving force transmission from the drum surface to the belt has not been thoroughly understood. These tests may be particularly important due to the new materials used for drum linings. One of the current design trends is to apply a new type of rubber-ceramic lining on drive drums [19].

Currently, the development of measuring equipment allows for determining the value of the actual coefficient of friction in variable industrial conditions, which in the future will enable designing a safer and more reliable drum friction drive.

In belt conveyors with a drum drive, the driving force is transferred to the belt thanks to the phenomenon of frictional contact. Striving to build long conveyors, the designers were forced to reduce the value of safety factors, use the belt's strength parameters more fully and reduce and constantly control the tension force at the minimum acceptable level. It was therefore necessary to better understand the phenomena taking place when the belt is going through the drive drum, in order to determine the conditions under which a slip between the belt and the drum occurred. The phenomenon of frictional contact is described by the Euler-Eytelwein dependence ($S_1 \leq S_2 \cdot e^{\mu\alpha}$), which has been known for more than 200 years, where variable parameters are belt-tensioning force S_2, drive drum's wrap angle α and friction coefficient μ [15]. The belt tensioning force is a parameter controlled by the tensioning system, the wrap angle depends on the geometric configuration of the drive drums, while the value of the friction coefficient is most often determined on the basis of tests carried out in laboratory conditions [25]. In fact, the value of the friction coefficient is a stochastic parameter, depending on, among

other things, the values of unit pressure and slip velocity, the condition of the surface of the friction pair, the type of intermediate layer or moisture. The measurement method used may also have a significant impact on the determined value of the friction coefficient.

This publication presents the results of laboratory investigations into the kinetic friction coefficient and an original method of its determination applied directly in the actual conditions of the belt conveyor's operation.

2. Preliminary laboratory tests

During the initial phase of the tests, the friction coefficient was determined in laboratory conditions for a clean and dirty belt, as well as a wet and dry belt, at low values of slip velocity, simulating the slip of the belt unwound on the drum surface, and at pressures corresponding to real conditions. The contamination was copper ore dust. Similar tests, in which the friction pair were spring elements and the results were the values of static and kinetic friction coefficients, have been presented in publication [8]. These tests took into account the different surface condition, different values of slip velocity and variable values of the normal load.

Laboratory tests of the friction coefficient between the belt cover and a fragment of the drum lining were carried out on a special stand (Fig. 1), which consists of a movable frame (1) with an attached and properly tensioned counter-sample (2). A counter-sample is a longitudinally cut tape having dimensions of 800x50 mm. In the stationary clamping system (3), there are mounted samples cut from the material of the drive drums lining in the form of two cubes (4), each of which has a contact surface of 20x20 mm. The drive system consists of an inverter-controlled gear motor (5) and a belt transmission. The frame is advanced by means of a screw and nut mechanism.

The friction coefficient tests were carried out for a fixed pressure force N=200N, tension P_1=P_2=2000N and slip velocity v=0,6mm/s. Before the actual tests, the running-in of the tape-lining friction pair
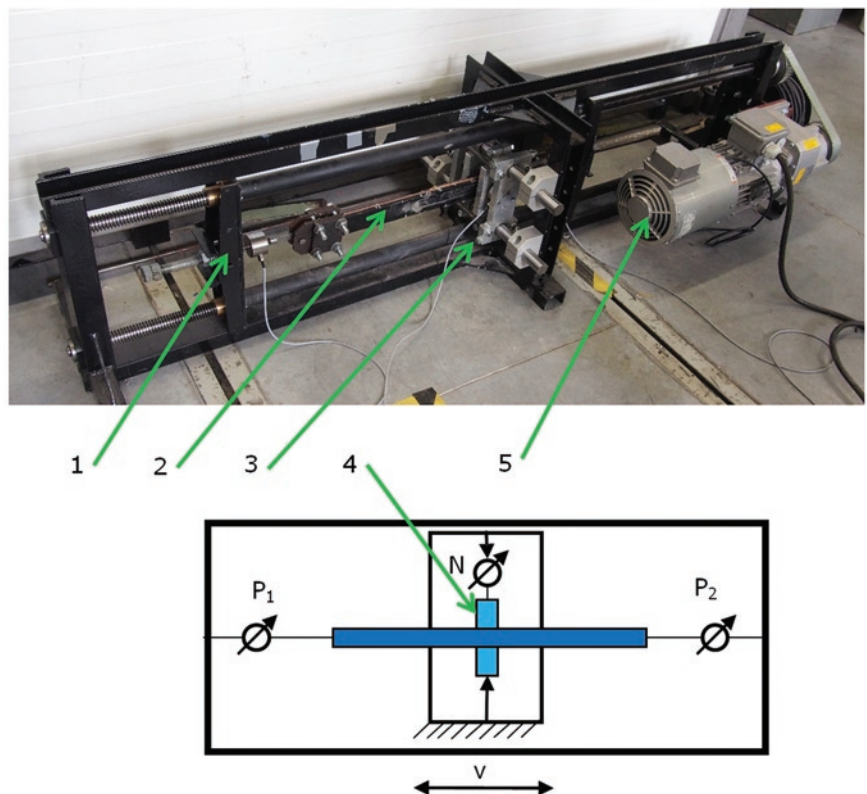

Fig. 1. View and schematic diagram of the stand for testing the friction coefficient [8]: 1 – movable frame, 2 - belt counter-sample, 3 – stationary sample clamping system, 4 - drum lining samples, 5 - drive
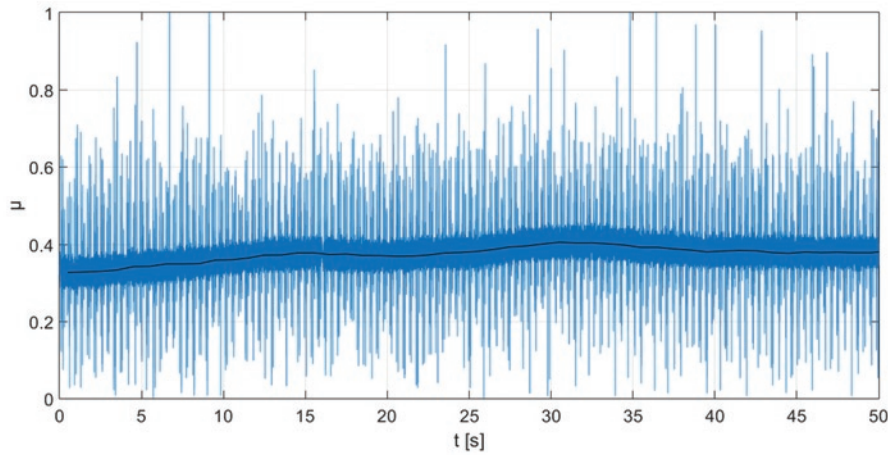
Fig. 2. Course of the friction coefficient for a wet and dust-contaminated friction pair [8]

(Fig. 3). Its value is determined on the basis of the following equation:

$$S_{\min} = \frac{g \cdot (m_t + m_u) \cdot l_g^2}{8 \cdot f_u} \quad [N] \quad (1)$$

where: m_t, m_u - unit masses of belt and mined rock, , [kg/m]; l_g – distance between upper idler sets, [m]; f_u- belt deflection between idler sets, [m]; g = 9,81 m/s².

The second condition, ensuring the correct frictional cooperation between the belt and the drum during start-up, is determined by the following dependence:

$$k_p \cdot P_N \le S_2\left(e^{\mu\alpha} - 1\right) \quad (2)$$

where: P_N- peripheral driving force, , [N]; k_p - slip protection factor, [-]; S_2 - force in the belt running off the drive drum , [N], α - drive drum's wrap angle, [rad]; μ - friction coefficient [-].

was performed over a length of approx. 50 mm to ensure stable friction conditions and repeatable results [10].

The tests were carried out many times for clean and contaminated samples, in both directions, while paying attention to the anisotropic nature of the friction phenomenon. An example of the changes in the friction coefficient during one of the tests is shown in Fig. 2

The value of the friction coefficient of the sample contaminated with dust from a finely ground copper ore determined during laboratory tests ranged from 0,37 to 0,53, depending on the degree of moisture and the direction of mutual movement of the samples and the counter-sample. The test results confirmed the random nature of changes in the friction coefficient value as well as the influence of the friction pair cooperation conditions and the method of conducting the measurement test on its value.

3. Characteristics of the operation of the drive-tensioning system

The aim of the research team was to determine the friction coefficient between the belt and the drum in industrial conditions. The necessary condition was to make the unrolled belt slip on the drum surface during the start-up of the belt, while simultaneously measuring the kinematic and dynamic parameters of the drive system. Determination of the belt slip conditions is facilitated by a diagram showing the characteristics of operation of the belt conveyor drive-tensioning system. This characteristic takes into account the features of the drive system and the tensioning device by presenting the required values of the belt tensioning force as a function of torque or driving force [13, 15].

3.1. Minimum values of the belt tensioning force

The value of the belt tensioning force for a given conveyor must be selected so that two conditions are met:
1) the belt sags between the idler sets of the upper and lower branches must be limited in order to maintain the proper geometric shape of the belt,
2) non-slip cooperation between the belt and the drum being driven or braked must be ensured.

The first condition is the minimum force in the belt assuming an acceptable belt sag. The most frequently assumed value is $f_u/l_g = 0{,}015$, and, during the braking of the belt, the quotient $f_u/l_g = 0{,}04$ is allowed [15]. This force does not directly depend on the driving torque, but only on the spacing of the idler sets and the transported masses
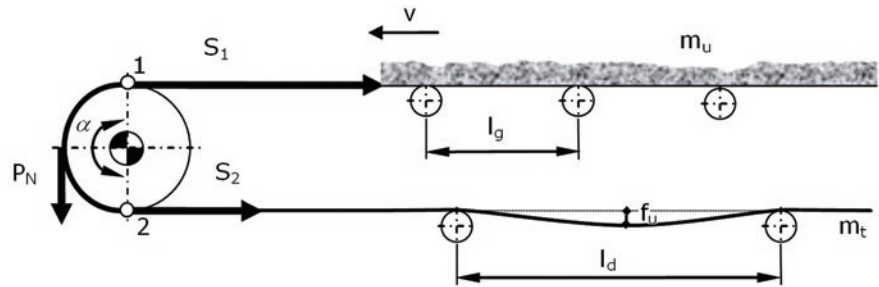

Fig. 3. Forces in the belt during drum driving

For a determined value of the peripheral driving force P_N, the tensioning device situated in the vicinity of the drive drum should ensure force S_2, defined by the following dependences:

$$S_2 \ge P_N \frac{k_p}{\left(e^{\mu\alpha} - 1\right)} \quad ; \quad S_2 \ge \frac{g \cdot m_t \cdot l_d^2}{8 \cdot f_u} \quad [N] \quad (3)$$

where: l_d - distance between lower idler sets, [m].

The value of wrap angle α for a given conveyor is constant, whereas the friction coefficient μ is a random variable. Assuming that the value of μ in the above relationships is constant and safe for particular conditions, we will obtain linear dependencies on the basis of which it can be concluded that the minimum forces S_2 which the tensioning device should induce in order to ensure the correct operation of the belt conveyor within the range $P \in [0; P_{Nmax}]$ are defined by lines a and b (Fig. 4).

Fig. 4 shows a set of values of force S_2 which are unacceptable during normal operation. A decrease in the value of the force in the (tensioning) belt running off the drive drum below line **b** may lead to the belt slip on the drum and result in the drum lining being worn and causing a fire hazard.

3.2. Actual characteristics of the conveyor belt tensioning device

Based on the calculated minimum values of the belt tension force according to the formulas: (1), (2) and (3), the required value of the
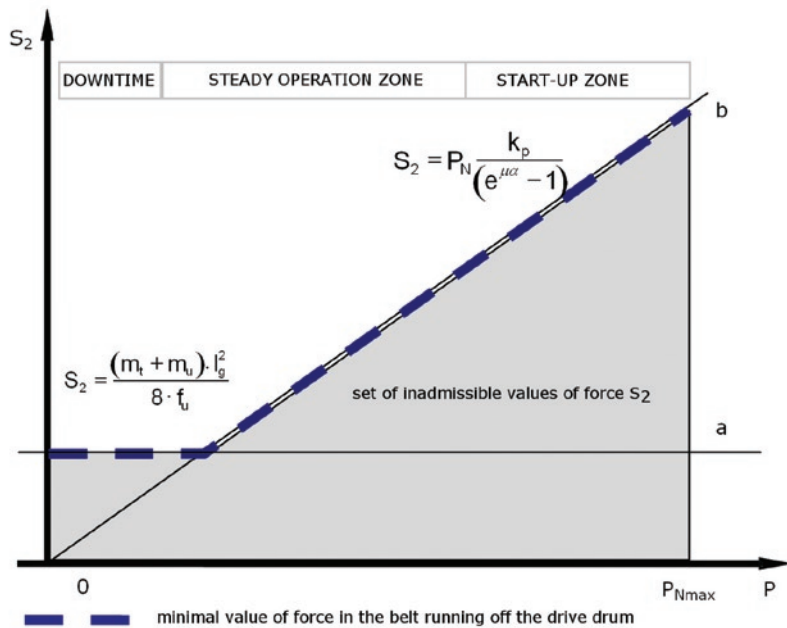
$$S_2 = P_N \frac{k_p}{(e^{\mu\alpha} - 1)}$$

$$S_2 = \frac{(m_t + m_u) \cdot l_g^2}{8 \cdot f_u}$$

set of inadmissible values of force S_2

— — minimal value of force in the belt running off the drive drum

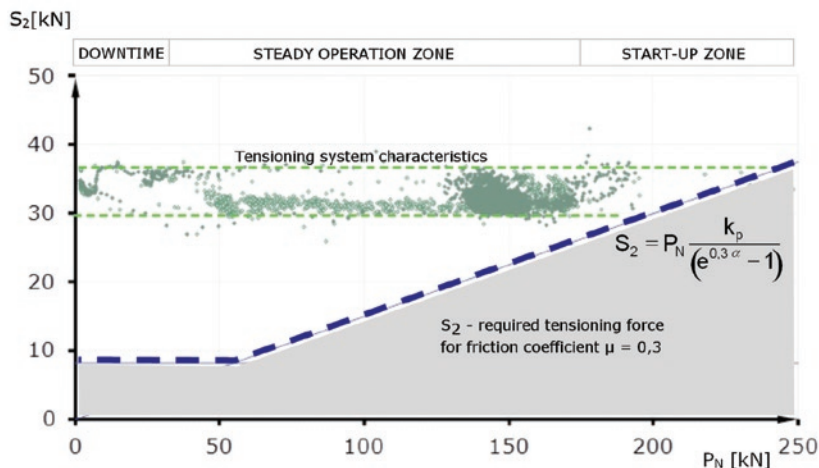Fig. 4. *Minimum values of the belt pre-tension force S_2 as a function of the driving force P on the driven drum*

$$S_2 = P_N \frac{k_p}{(e^{0,3\alpha} - 1)}$$

S_2 - required tensioning force for friction coefficient $\mu = 0,3$

Fig. 5. *Operational characteristics of the drive-tensioning system with a gravity tensioning device, determined on the basis of measurements*

force in the belt running off the drive drum as a function of the driving force is determined. Next, the characteristics of tensioning devices, obtained on the basis of calculations, simulation and laboratory or industrial tests [13], are placed on a simplified diagram showing these dependencies (Fig. 2).

Fig. 5 below shows an example of the actual characteristics of the tensioning device obtained on the basis of the results of a series of measurements of forces in the conveyor belt during start-ups, steady operation and braking of the conveyor belt. The belt conveyor was equipped with a gravity belt tensioning system, located just behind the main conveyor drive. The belt tensioning force was in the range of 29 ÷ 37 kN. Fluctuations in this force were caused by the inertia of the weights and the efficiency of the tensioner system.

The diagram of the permissible, minimum forces in the belt presented in Fig. 5 indicates that the drive will work non-slip with the actual characteristics of the gravity tensioning system. The necessary condition is to use drum linings and effective cleaning devices ensuring a minimum value of the friction coefficient μ=0,3.

The actual characteristics of the tensioning system shown in Fig. 5 were recorded in industrial conditions, using a mobile measuring system described in Chapter 4.

4. Industrial tests

A typical mining belt conveyor that transports copper ore was selected for industrial measurements of the friction coefficient between the drum lining and the conveyor belt. The measuring system described below, intended for the testing of industrial belt conveyors, meets the requirement of measuring stations' mobility and non-invasiveness, which was set at the design stage. The mobility of the stations enables installing them on the conveyor on the day of measurements as well as preparing for data recording in no more than 2 hours. (installation of measuring equipment, sensors, recorders, checking the correct operation of measurement chains). On the other hand, non-invasiveness of the measuring system ensures that none of the conveyor components will be modified or replaced, and that the tested belt conveyor can at any time resume its standard transport task. Moreover, it has been assumed that all measured physical quantities will be registered simultaneously and each of the data acquisition points of the measuring system will be powered autonomously.

A non-invasive mobile measuring system in its basic configuration includes three stations that record measurement signals during start-up, steady operation under variable load and during the conveyor's braking. One station, recording the speed of the upper and lower belt as well as the feed efficiency, is located on the conveyor route, the second one is in the electrical switchboard, and the third one is placed in the area of the conveyor's drive and tensioning system. Measurement data from this stand was used to verify the actual value of the friction coefficient between the belt and the surface of the drive drum.

The measuring station for the drive and tensioning system, shown in Fig. 6, is located in the area of the drive and tensioning station. The station is equipped with a box with a battery power supply system, a measuring computer, sensors for measuring the force in the belt and line, a set of belt speed sensors and optical rotational speed sensors.

During measurements, it is possible to observe and record changes in the following parameters:
– xA,xB - belt displacement at stations A and B [m],
– vA,vB - belt speed at stations A and B [m],
– xl - rope displacement in the belt tensioning system [m],
– SL - force in the stationary line of the belt tensioning system [kN],
– RA,RB - reaction forces on the deflecting drums of the measuring system A, B [kN]
– n - rotational speeds of drive motors shafts, high-speed shafts of gears or drum [rpm].

Based on the measured parameters, the following are determined:
– STN,STZ - forces in the belt at stations A and B, i.e. in the area where the belts run onto or off the drive drums [kN],
– s - the actual safety factor [-],
– P - peripheral driving force on the drive drums, balancing the resistance to the conveyor's movement W [kN],
– M - driving torque in drive units equipped with hydrodynamic couplings having known characteristics [Nm],
– N - drive power [kW],
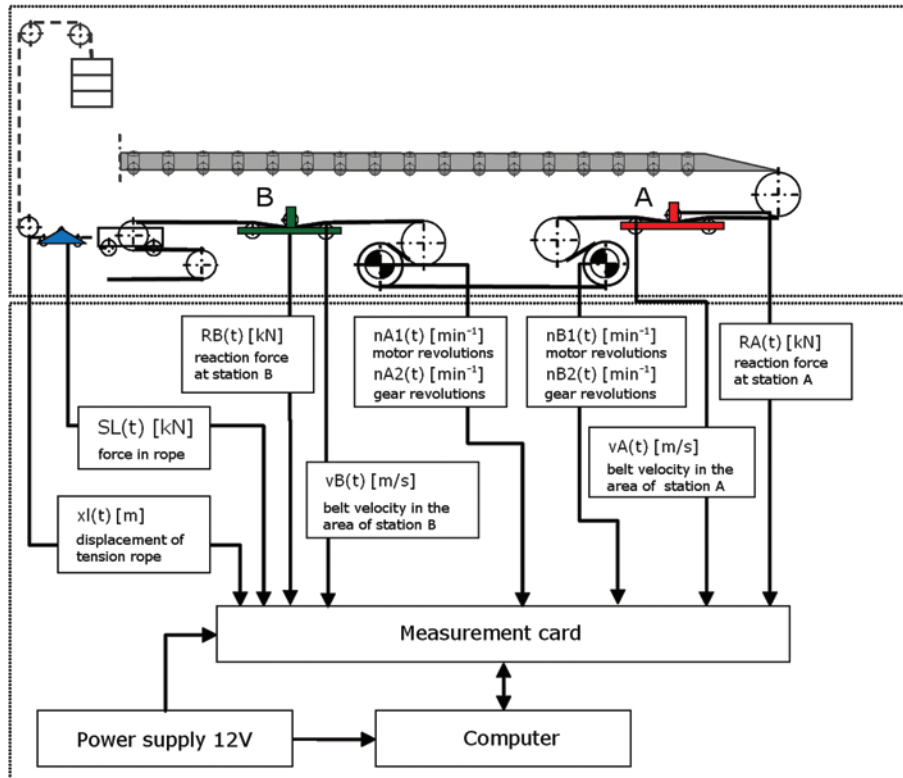– xw - stroke of the belt tensioning trolley [m],

Fig. 6. Diagram of the measuring chains of the complete measuring system of the drive-tensioning system
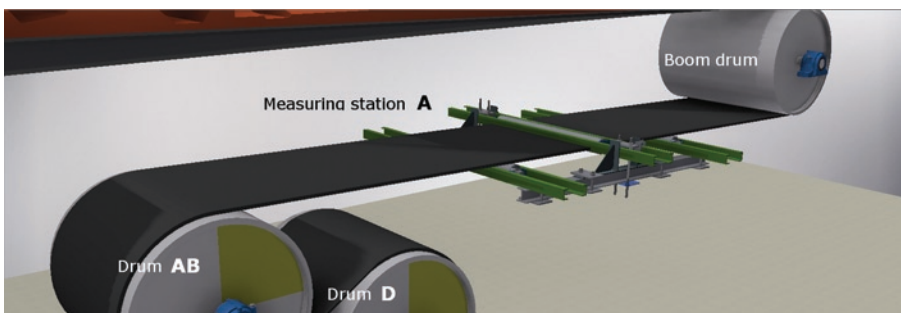

Fig 7. Stand A for measuring the force in the belt running on the drive drums

STN - force measured in the belt running onto the drive drum AB [kN]

STM - calculated force in the belt between drums [kN], STM=STZ+P_D

STZ – force measured in the belt running off the drive drum D [kN]

Fig. 8. Diagram of the tested conveyor and location of measuring points

– vw - speed of the belt-tensioning trolley [m / s],
– η - efficiency of the tensioning system [-],
– μ- friction coefficient between the belt and the drive drum surface [-].

Fig. 7. shows the visualization of the installation of measuring station A in the area where the belt runs onto the drum drive system.
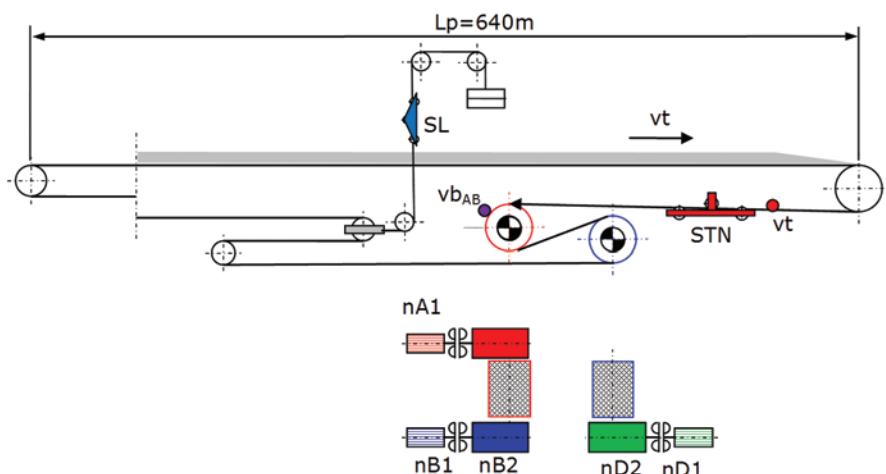
The industrial tests were carried out on a belt conveyor with a gravity belt tensioning system and a two-drum drive system, equipped with three motors and hydrodynamic starter couplings installed in accordance with the diagram in Fig. 8.

Technical and operational parameters of the tested conveyor:

• Conveyor's length : L = 640 m,
• Belt speed: v = 2,73 m/s,
• Average inclination angle of the conveyor route:δ = 2,87°,
• Type of tensioning device: gravity.

During the measurements, a series of start-ups of the conveyor was carried out with variable load of the handled material and for different sequences of switching on motors A, B, D. Among others, the following were recorded: belt speed in the drive area, forces in the belt running onto the drive system (STN) and in the tensioning system line (SL), rotational speed of the motor shafts (nA1, nB1, nD1) and gears (nB2, nD2) and peripheral speed of drum AB (vb$_{AB}$) - Fig. 8.

The measurement results were used, among others, to determine the friction coefficient between the belt and the lining of the drive drum

Fig. 9. Diagram of a two-drum drive system

coefficient between the belt and the lining of the drive drum AB. The delay in turning on motor D resulted in a macro-slip on drive drum AB.

The conveyor was started up according to the following sequence: start-up of motor A, after 0,7 s start-up of motor B and, after seven seconds, start-up of motor D. The belt speed and the peripheral speed of the drum were recorded using a mobile measuring system.

The difference between the values of the belt speed vt and the peripheral speed of the drum vb_{AB} represents the belt slip on the drum (Fig. 10). The slip began after approx. 1,5 s from the
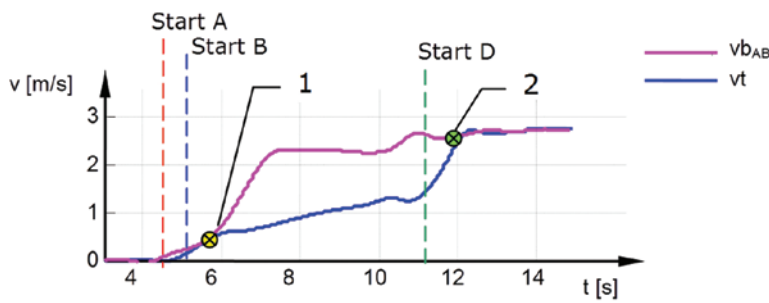

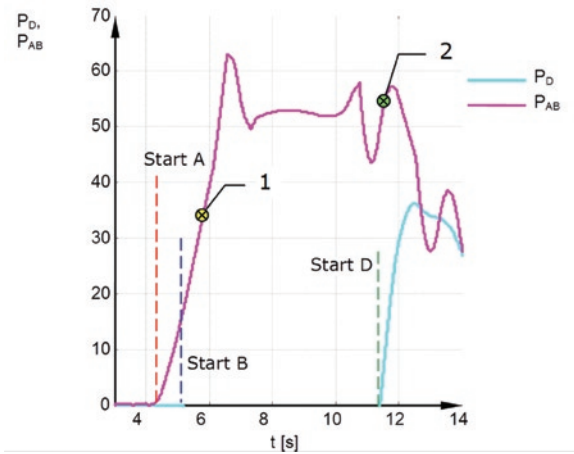Fig. 10. Method of measuring the belt speed vt and the peripheral speed of the drum vb_{AB}

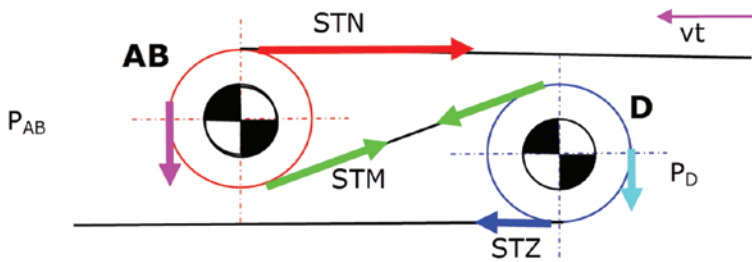Fig. 13. Course of changes in the peripheral force on drums AB and D.

Fig. 11. Course of changes in the belt speed vt and the peripheral speed of the drum vb_{AB}

The case of a slip between the belt and the drum during start-up was analysed.

The possibility of changing the sequence of switching on motors A, B, D allowed for an experiment that involved determining the friction

start-up of motor A (Fig. 11 - point 1), lasted about 6 seconds and ended after increasing the belt tension, when motor D was started up (Fig. 11 - point 2).

The course of changes in the peripheral driving force for drums AB and D was determined on the basis of the recorded courses of changes in the slip of the coupling (Fig. 12) and the knowledge of hydrodynamic couplings characteristics, which enable calculating the torque of the coupling M_s. The characteristics of hydrodynamic couplings were determined in the laboratory of their manufacturer. The knowledge of the driving force $P_D=M_s*i/R_{AB}$ and the force in the STZ belt running off the drive drum enabled determining the force in the belt between the drive
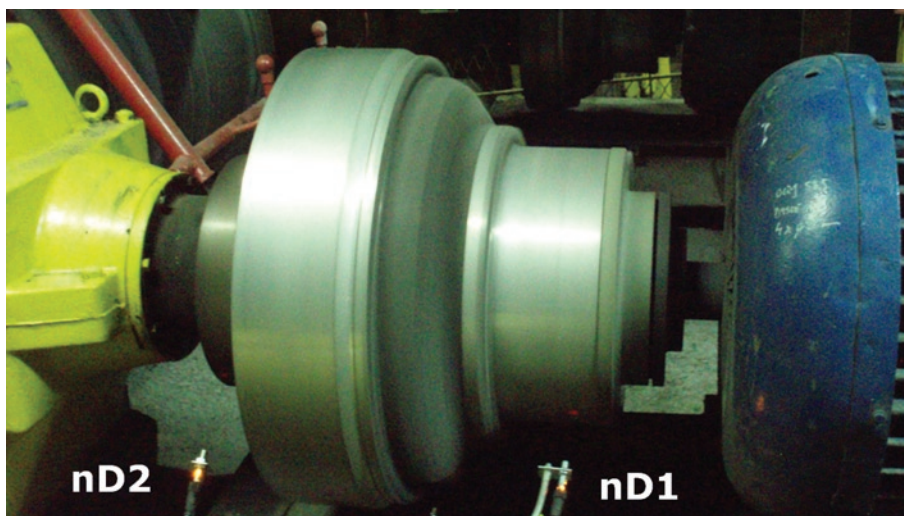

Fig. 12. Measurement of the rotational speed of the pump and turbine part of the hydrodynamic coupling
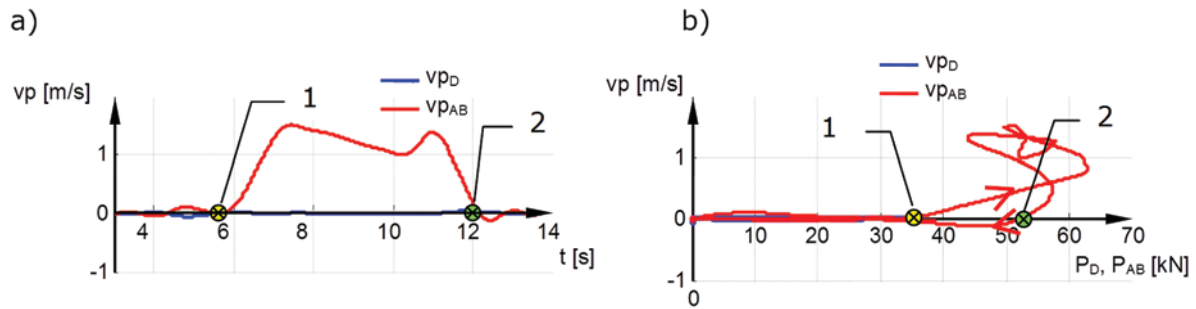
Fig. 14. Course of changes in the speed of belt slip drum AB - vp_{AB} and D - vp_Dw versus time (a) and as a function of peripheral force on drive drums (b)

drums $STM = P_D + STZ$ (Fig.9). The course of changes of this force is shown in Fig. 16a.

Fig. 15. Method of measuring the force in the STN belt at station A

The course of the peripheral driving force for drums AB and D is shown in Fig. 13. Points 1 and 2 mark the beginning and end of the slip on drum AB.
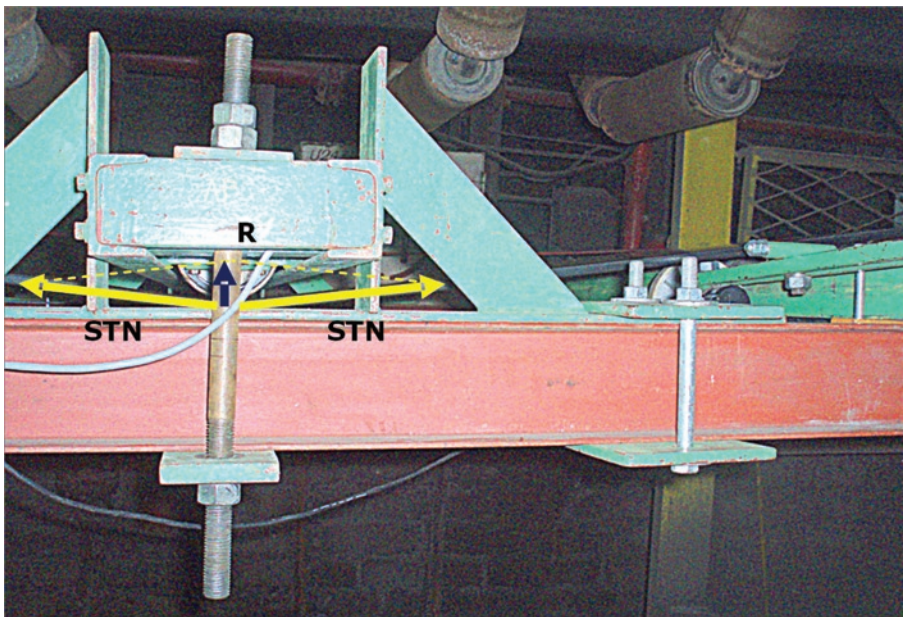
Determination of the beginning and end of the slip phase enabled presenting the changes in the belt slip speed on drums AB and D as a function of the determined peripheral driving force (Fig. 14b). Slip speed is the difference between the peripheral speed of the drum and the speed of the belt ($vp_{AB}=vb_{AB}$-vt). It can be read from the diagram that the belt slip on drum AB started with a driving force of approx. 34 kN and ended at approx. 53 kN. There was no slip on drum D.

The force in the belt running onto drive drums - STN was determined on the basis of measurements of the value of the reaction force acting on the roller deflecting the belt run (Fig. 15). The force in the belt running off the drive drum was calculated on the basis of measurements of the force in the line of the SL belt tensioning system (Fig. 8).

The knowledge of the force in the belt between the drive drums - STM and the peripheral driving force - P_{AB} allowed for presenting the characteristics of the drive-tensioning system for drum AB. Figure 14b shows the actual characteristics of the drive-tensioning system and the values of the tensioning force for the friction coefficient in the range of 0,1 ÷ 0,5, which
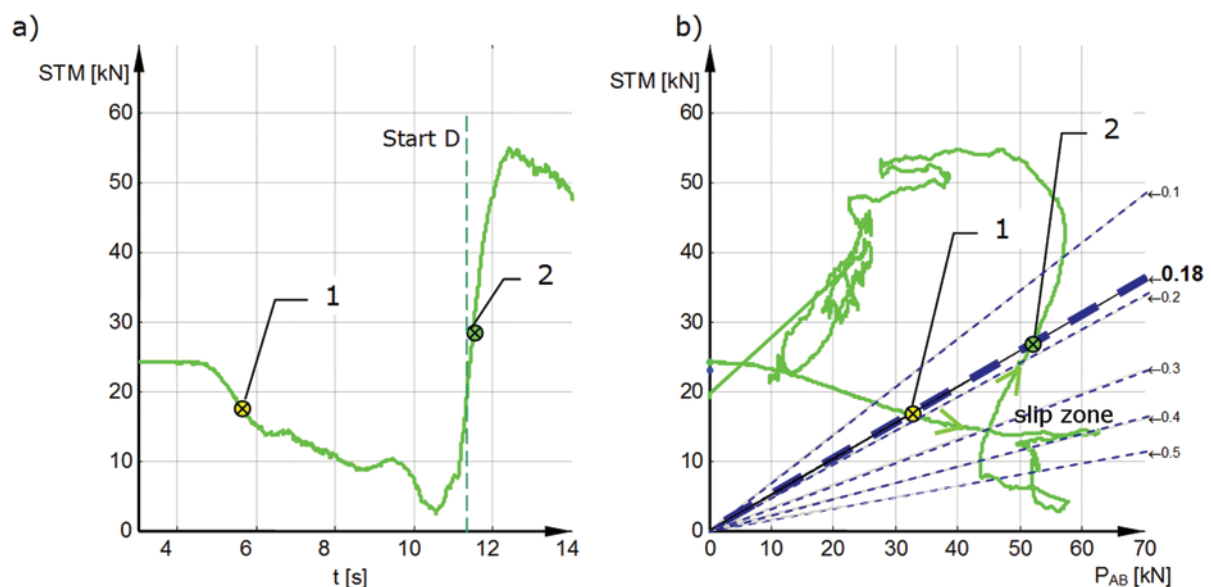

Fig. 16. Course of changes of the force in the belt between the drums during STM start-up versus time (a) and as characteristics of operation of the drive-tensioning system for drive drum AB (b)

Fig. 17. Condition of the drive drum lining during the tests

are required due to the anti-slip protection. The required values of belt tension are marked with dotted lines (Fig. 14b).

The characteristics of the drive-tensioning system (Fig. 16b) have been marked with points representing the beginning (1) and the end of the belt slip (2), taking into account the course of changes in the tensioning force versus time (Fig. 16a) as well as the values of the driving force P_{AB} that mark the beginning and end of the slip (Fig. 12b item 1 and item 2). The straight line passing through these points corresponds to the required tensioning force determined for the friction coefficient μ=0,18.

The value of the coefficient of friction between the contaminated belt lining and the lining of drive drum AB, determined by the indirect measurement method in industrial conditions, was μ=0,18 at the time of slip. It is a value below the level required for designing a conveyor (μ>0,25), but seems probable considering the operating conditions of the conveyor and the condition of the drum lining (Fig. 17.)

5. Summary

The mobile, non-invasive measuring system of belt conveyors and the measuring equipment as well as the appropriate procedures applied proved to be fully suitable for measurements performed in underground mines. The results of measurements can be used for diagnostic purposes. They can demonstrate the correct operation of conveyors, but also indicate errors in design assumptions, calculations and selection of conveyor components, resulting in reduced durability of components and lower reliability of the conveyor, which translates into increased operating costs. An important task for the mobile meas-

urement system is verification of the applied calculation models and selected calculation factors. The conducted industrial tests allowed for extending the scope of calculations of programs supporting the design process and enabled validation and improvement of models used to analyse dynamic phenomena occurring during the operation of the conveyor [13, 14, 15].

As part of the research presented in this publication, the actual performance characteristics of the mining belt conveyor drive and tensioning system were determined. These characteristics illustrated the case of the conveyor start-up in a situation when a slip occurred between the belt and the drive drum. Based on the characteristics, the actual limit value of the friction coefficient between the belt and the drum lining was estimated, which in this case reached μ=0,18. The low value of the coefficient is most likely caused by the high degree of wear and contamination of the drive drum lining.

The value of the kinetic friction coefficient determined in laboratory conditions proved to be more than twice higher than the value obtained during industrial measurements. This indicates that it is difficult to perform repeatable and reliable tests of the kinetic friction coefficient for friction pairs used in drive systems. The rubber lining of the drum and the belt work in conditions of high pressure, significant contamination and moisture, which causes their accelerated abrasion and wear. The problem of belt slip on the drive drum of the test conveyor was solved by accelerating the start-up of motor D, which resulted in an increase in the force in the belt running off drum AB and a correct start-up of the conveyor.

References

1. Andrejiova M, Grincova A, Marasova D. Analysis of tensile properties of worn fabric conveyor belts with renovated cover and with the different carcass type. Eksploatacja i Niezawodnosc - Maintenance and Reliability 2020; 22(3): 472-481, https://doi.org/10.17531/ein.2020.3.10
2. Gładysiewicz L, Król R, Kisielewski W. Measurements of loads on belt conveyor idlers operated in real conditions. Measurement: Journal of the International Measurement Confederation 2019; 134: 336-344, https://doi.org/10.1016/j.measurement.2018.10.068.
3. Gładysiewicz L, Kawalec W, Król R. Selection of carry idlers spacing of belt conveyor taking into account random stream of transported bulk material. Eksploatacja i Niezawodnosc - Maintenance and Reliability 2016; 18(1): 32-37, https://doi.org/10.17531/ein.2016.1.5.
4. Gładysiewicz L, Kró, R, Kisielewski W, Kaszuba D. Experimental determination of belt conveyors artificial friction coefficient. Acta Montanistica Slovaca 2017;22(2): 206-214.
5. Goncharov KA, Grishin AV. Theoretical study of influence of belt tension of intermediate belt conveyor drive on value of zone of relative slip of traction and carrying belts. IOP Conference Series: Earth and Environmental Science 2017; 87(2): 022008, https://doi.org/10.1088/1755-

1315/87/2/022008.

6. Halepoto IA, Shaikh MZ, Chowdhry BS, Uqaili Muhammad A. Design and Implementation of Intelligent Energy Efficient Conveyor System Model Based on Variable Speed Drive Control and Physical Modeling. International Journal of Control and Automation 2016; 9(6): 379-388, https://doi.org/10.14257/ijca.2016.9.6.36.

7. Harrison A. A comparison of friction models for conveyor design. 9th International Conference on Bulk Materials Storage, Handling and Transportation, ICBMH 2007.

8. Hryciów Z, Krasoń W, Wysocki J. The experimental tests on the friction coefficient between the leaves of the multi-leaf spring considering a condition of the friction surfaces. Eksploatacja i Niezawodnosc - Maintenance and Reliability 2018; 20(4): 682-688, https://doi.org/10.17531/ein.2018.4.19.

9. Jurdziak L, Blazej R, Bajda M. Conveyor belt 4.0. Advances in Intelligent Systems and Computing 2019; 835: 645-654, https://doi.org/10.1007/978-3-319-97490-3_61.

10. Kasza P, Kulinowski P, Zarzycki J. The Influence of an Operating Conditions on the Friction Coefficient in Transportation Machines Drives. New Trends in Production Engineering 2020; 3(1): 294-302, https://doi.org/10.2478/ntpe-2020-0024.

11. Król R. Studies of the Durability of Belt Conveyor Idlers with Working Loads Taken into Account. IOP Conference Series: Earth and Environmental Science 2017; 95(4): 042054, https://doi.org/10.1088/1755-1315/95/4/042054.

12. Król R, Kisielewski W. Research of loading carrying idlers used in belt conveyor-practical applications. Diagnostyka 2014; 15 (1): 67-73.

13. Kulinowski P. Simulation method of designing and selecting tensioning systems for mining belt conveyors. Archives of Mining Sciences 2014; 59(1): 123-138, https://doi.org/10.2478/amsc-2014-0009.

14. Kulinowski P. Simulation studies as the part of an integrated design process dealing with belt conveyor operation. Eksploatacja i Niezawodnosc- Maintenance and Reliability 2013; 15 (1): 83-88.

15. Kulinowski P. Analytical method of designing and selecting take-up systems for mining belt conveyors. Archives of Mining Sciences 2013; 58(4): 1301-1315, https://doi.org/10.2478/amsc-2013-0090.

16. Kulinowski P, Kasza P, Zarzycki J. The methodology of testing rotational resistances of the rollers under the operation load. New Trends in Production Engineering 2019; 2(1): 337-343, https://doi.org/10.2478/ntpe-2019-0036.

17. Mazurkiewicz D. Computer-aided maintenance and reliability management systems for conveyor belts. Eksploatacja i Niezawodnosc- Maintenance and Reliability 2014; 16(3): 377-382.

18. Mazurkiewicz D. Analysis of the ageing impact on the strength of the adhesive sealed joints of conveyor belts. Journal of Materials Processing Technology 2008; 208(1-3): 477-485, https://doi.org/10.1016/j.jmatprotec.2008.01.012.

19. Patton PW, Smith CS. Toward an effective friction factor for ceramic-in-rubber pulley lagging: An analysis of field data. Bulk Material Handling by Conveyor Belt V. 2004; 107-109.

20. Satria I,Rusli M. A Comparison of Effective Tension Calculation for Design Belt Conveyor between CEMA and DIN Standard. MATEC Web of Conferences 2018; 166: 01007, https://doi.org/10.1051/matecconf/201816601007.

21. Walker P, Doroszuk B, Król R. Analysis of ore flow through longitudinal belt conveyor transfer point. Eksploatacja i Niezawodnosc - Maintenance and Reliability 2020; 22 (3): 536–543, https://doi.org/10.17531/ein.2020.3.17.

22. Wenrong W, Jianhua Q, Wangheng. Research on the influence of tensioning device in the dynamic process of belt conveyor. ACM International Conference Proceeding Series 2018; 186-190, https://doi.org/10.1145/3305275.3305312.

23. Wheeler C, Munzenberger P, Ausling D, Beh B. How to design energy efficient belt conveyors. Bulk Solids Handling 2015; 6: 40-50.

24. Woźniak D. Laboratory tests of indentation rolling resistance of conveyor belts. Measurement: Journal of the International Measurement Confederation 2020; 150: 107065, https://doi.org/10.1016/j.measurement.2019.107065.

25. Zakharov A, Gerike B, Shiryamov D. The Ultimate Rotating Resistance of the Belt Conveyors Rollers 2018; 176: 227-230, https://doi.org/10.2991/coal-18.2018.42.

26. Zimroz R, Hardygóra M, Blazej R. Maintenance of Belt Conveyor Systems in Poland – An Overview 2015: 21-30, https://doi.org/10.1007/978-3-319-12301-1_3.